Quantum Electronics **37** (4) 325 – 330 (2007) ©2007 Kvantovaya Elektronika and Turpion Ltd

PACS numbers: 42.55.Lt; 42.60.Lh; 52.20. – j; 52.25. – b
DOI: 10.1070/QE2007v037n04ABEH013203

Study of the dependence of the specific output power of a copper chloride laser on the radial temperature profile of a gas plasma

R. Sadighi-Bonabi, F. Soltanmoradi, R. Mohammadpour, M. Tavakoli, M. Zand

***Abstract*. The design of a copper chloride laser is described, and the laser is optimised by studying the dependence of its output power on the buffer gas type. The voltage and current of the laser discharge at the optimum buffer gas pressure are measured. The influence of the diaphragm diameter on the specific output power is studied after optimisation of switch parameters. When an diaphragm producing the optimal temperature gradient in the laser gas-discharge tube, the record specific output power of 123 W L^{-1} is obtained without any admixtures.**

Keywords: *copper chloride laser, buffer gas, radial temperature profile, specific output power.*

1. Introduction

Since the first demonstration of a copper vapour laser (CVL) in 1966 [1], its output power has been increased from 20 mW for a pulse repetition rate of 600 Hz and the discharge tube of diameter 1 cm to more than several hundreds of Watts in a broad range of repetition rates from 1 to 100 kHz and efficiencies of more than 1% [2]. Copper vapour lasers have found a variety of applications in medicine (dermatology and photodynamic therapy), science and technology (pumping dye lasers for various applications, including isotope separation, etc.) [3, 4].

Various optimisation methods have been proposed to increase the power and efficiency of CVLs [5 – 8]. However, to obtain high output powers and efficiencies of CVLs, it is necessary to produce the optimum operation temperatures of about 1500 °C, which involves many technical problems. In particular, when a master oscillator – power amplifier (MOPA) system is used, for example, for atomic vapour isotope separation (AVLIS), these discharge-pumped lasers require a rather long time of about 45 minutes to heat the gas-discharge tube and another 45 minutes to obtain the maximum output power.

R. Sadighi-Bonabi, R. Mohammadpour, M. Tavakoli Physics Department, Sharif University of Technology, P.O.Box: 11365-9161, Tehran, Iran; e-mail: sadighi@sharif.ir;
F. Soltanmoradi Bonab Research Center, P.O.Box: 56515-196, Bonab, Azerbaijan province, Iran;
M. Zand Laser Research Center, AEOI, P.O.Box: 11365- 8486, Tehran, Iran

Received 21 February 2006; revision received 27 June 2006
Kvantovaya Elektronika **37** (4) 325 – 330 (2007)
Submitted in English

To overcome this disadvantage, the copper halide compounds were used, which could be vaporised at lower temperatures from about 400 °C to 600 °C depending on the copper halide type. As a result, it takes less than 10 minutes to start lasing.

Despite this advantage, a disadvantage of copper halide vapour lasers (CHVLs) is that the beam diameter of this laser is smaller than the active-volume diameter, which was pointed out by many authors [8 – 10]. This is related to the low electron and gas temperature near the tube wall, whereas to obtain a uniform discharge, it is necessary to maintain high electron temperature over the entire tube diameter. The inverse population in CVLs and CHVLs is produced by pulsed electric current systems, which are similar to those used in other metal vapour lasers (for example, gold, lead and manganese vapour lasers). The self-terminating transitions from the resonance (r) to metastable (m) level play an important role in the formation of transient inversion in metal vapour lasers. Figure 1 shows the excitation rate constants of the r and m levels of copper atoms, calculated from their cross sections by assuming that the electron energy distribution function (EFDL) is Maxwellian [11]. One can see from Fig.1 that the threshold electron temperature T_e for the excitation rate of the r level is 1.54 eV. Therefore, to pump a CVL efficiently, the field in the plasma (which determines the value of T_e) should be rather strong almost immediately after the onset of the excitation pulse, i.e. the voltage pulses should have a steep leading edge, which was experimentally confirmed in [9].

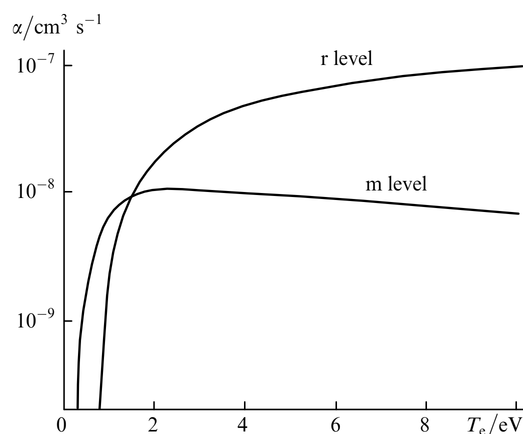

Figure 1. Dependences of the excitation rate constants for the resonance (r) and metastable (m) levels of the copper atom on the electron temperature.

1.1 Hydrogen addition

The improvement of the emission parameters of CVLs and particularly CHVLs after the addition of small amounts of hydrogen was reported in many papers [12–15]. The performance of CuBr–H lasers was compared with that of the HyBrID (Hydrogen Bromide in Discharge) lasers [16]. The improvement in the efficiency and certain features of the current and voltage pulses can be explained by the dissociative attachment of cold electrons to HBr molecules. This process can be schematically represented in the form:

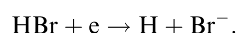

$$\mathrm{HBr} + \mathrm{e} \rightarrow \mathrm{H} + \mathrm{Br}^{-}.$$

The cross section of this process for the electron energy of 0.28 eV is 2.7×10^{-16} cm^2 and decreases rapidly with increasing the electron energy [16]. This process reduces prepulse concentration of electron and copper atoms in the metastable state and weakly affects high-energy electrons. This favours excitation of the resonance level rather than the metastable level, resulting in the increase in the output power and efficiency.

Note that the addition of hydrogen causes some adverse effects such as greater consumption of energy supplied to the plasma during the excitation pulse, dissociation and vibrational excitation of molecular hydrogen. In addition, due to the energy release during the thermalisation of vibrationally excited hydrogen molecules, the plasma relaxation between two pulses slows down [15]. Other problems appearing upon addition of hydrogen are related to a particular CHVL type, for example, the influence of electron attachment to the HCL molecule is considerably less than for HBr and HI molecules [9].

1.2 Other methods

In recent years some other methods for increasing the CVL efficiency have been investigated. Chang studied the plasma kinetics in CVLs by using a genetic algorithm and proposed to remove cold electrons from the active volume upon the laser pumping, i.e. to maintain a high wall temperature to increase the inverse population [7]. Although in this case the electron and gas temperature in the discharge remains high, a sharp temperature drop still exists across the gas-discharge tube. It is rather difficult to reduce the temperature gradient in the entire working volume.

In this work, quartz diaphragms were used to isolate the cold regions near the tube walls from the active discharge volume. For this purpose, a copper chloride laser was constructed and the effect of different buffer gases on the output power was investigated. After determining the optimal operating pressure for different buffer gases, the voltage, current and laser pulses were measured. The discharge region was confined to some extent by using diaphragms with different diameters. The specific output power was measured and the radial profile of the plasma temperature was calculated. Finally, by optimising these parameters, we determined the exact copper chloride vapour pressure by adjusting the distance between the discharge axis and radiation source, and selected the switch parameters. This allowed us to obtain the maximum specific output power of 123 W L^{-1}. This is the highest specific output power achieved in CHVLs with the bore diameter exceeding 1 cm without using any admixtures such as hydrogen.

2. Experimental

Figure 2 shows the scheme of the CuCl laser constructed in this work. The discharge tube was made of 80-cm long fused silica tube with the internal diameter of 20 mm. The distance between electrodes was 30 cm. Four quartz diaphragms at the same distance from each other were placed inside the tube. Three grams of copper chloride, necessary for the 20-hour operation of the laser, were placed in a special container located in a 10-cm arm at the center of the tube between the electrodes. Because of the long distance between the radiation source and the discharge axis, it was necessary to control the CuCl vapour pressure with the reservoir heater (independently of the temperature produced by the discharge tube). Two cold traps located between the electrode and a BK7 glass window were used to prevent contamination of laser windows by inhibiting diffusion of vapour onto the windows. The laser tube was wrapped with the insulation whose thickness depended on the electric discharge power. The laser cavity consisted of two flat mirrors: a 99 % highly reflecting mirror and an 8 % reflection output coupler. The temperature of the outside wall of fused silica tube was controlled continuously with an Hg thermometer which was fixed to the outside wall. Because of electronic shock hazard and very high RF noise generated by the experimental equipment, we did not use an electronic thermometer. The partial gas pressure under the optimum operating condition was 0.3 Torr for CuCl and 30 Torr for Ne.

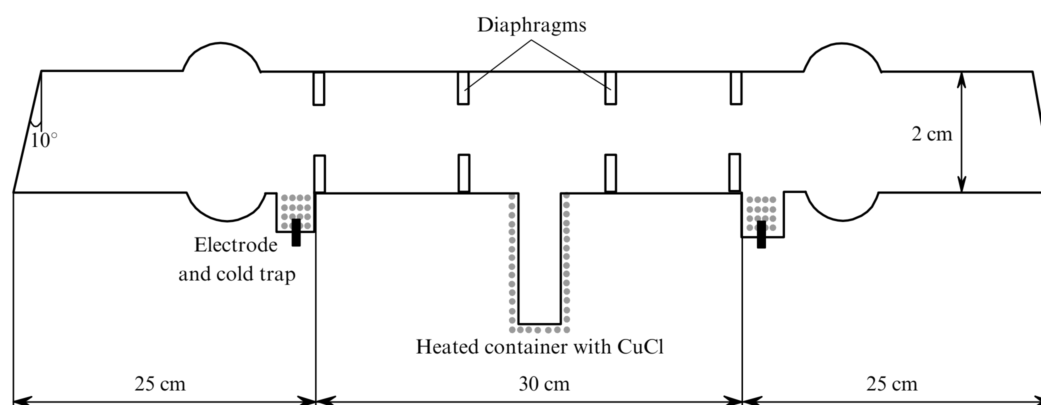

Figure 2. Scheme of the cross section of sealed-off fused-silica tube of a CuCl laser.

The selection of the pump parameters of lasers is governed by the stable operation of thyratron, which is controlled with the reverse negative voltage on the thyratron anode. Stable laser operation can be provided by selecting properly circuit parameters, which include the low inductance of the thyratron and the gas-discharge tube (GDT) and the optimum capacity of the storage capacitor [17–19]. We used this approach many years ago to optimise the XeCl laser. We found the main factors which limit the maximum allowable values of the thyratron rise rate and the reverse voltage across the thyratron [20, 21]. In this paper, the optimum matching of the circuit parameters with the wave impedance was achieved by dischrging a 1.1-nF storage capacitor through an air-cooled low inductance TGI1-1000/25 thyratron; a 0.5-nF peaking capacitor and a 174-μH by-pass inductor were connected parallel with the tube. The current, voltage and laser pulses were measured with a 200-MHz Tektronix TDS2024 oscilloscope.

3. Experimental results

The rise time of the voltage pulse across the GDT in our experiments decreased with increasing the natural oscillation frequency. This was achieved by optimising the circuit parameters as discussed above. The effects of different buffer gases and vapour pressures were studied. When the optimum conditions were achieved, the output power was optimised by inserting suitable diaphragms.

3.1 Buffer gases

The effect of different types of buffer gases (Ne, He, Ar) on the output power was examined by recording the voltage, current and laser pulse oscillograms. Figure 3 shows the dependence of the output power on the buffer gas pressure. One can see that the choice of the buffer gas significantly affects the output power. Thus, no lasing was observed when Ar was used as a buffer gas.

Figures 4, 5 and 6 show the typical voltage, current and laser pulses in the presence of different buffer gases at their optimum pressure. It is found that when He is used instead of Ne as a buffer gas, the peak current significantly decreases from 150 A (Fig. 4) to 90 A (Fig. 5). Therefore, the plasma tube resistance increases when He is used. This happens for two reasons:

(i) The ionisation potential of He (24.59 eV) is much higher than that of Ne (21.56 eV), which, in the case of He, yields fewer electrons in an equal electric field.

(ii) The atomic weight of He is less than that of Ne, so the rate of the energy transfer in elastic electron collisions is

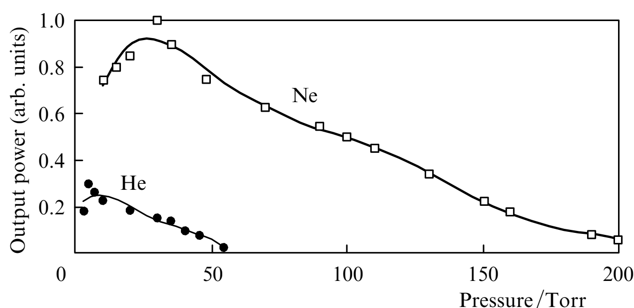

Figure 3. Dependences of the output power on the He and Ne buffer gas pressures.

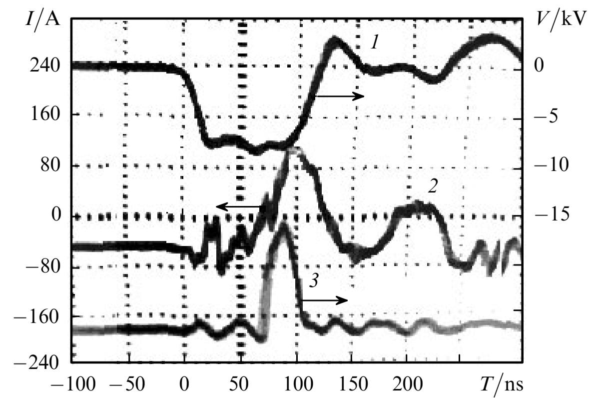

Figure 4. Voltage (*1*), current (*2*) and laser (*3*) pulse oscillograms for a 13-mm bore, 30-cm long CuCl-laser tube at a Ne buffer gas pressure of 30 Torr.

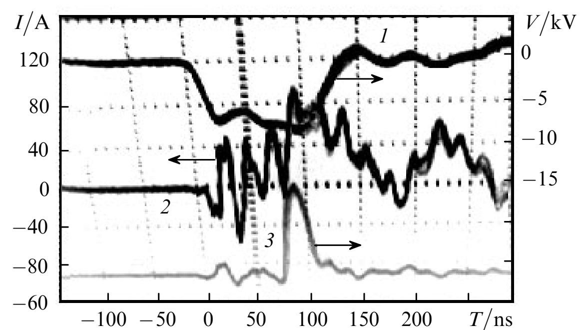

Figure 5. Voltage (*1*), current (*2*) and laser (*3*) pulse oscillograms for a 13-mm bore, 30-cm long CuCl-laser tube at a He buffer gas pressure of 5 Torr.

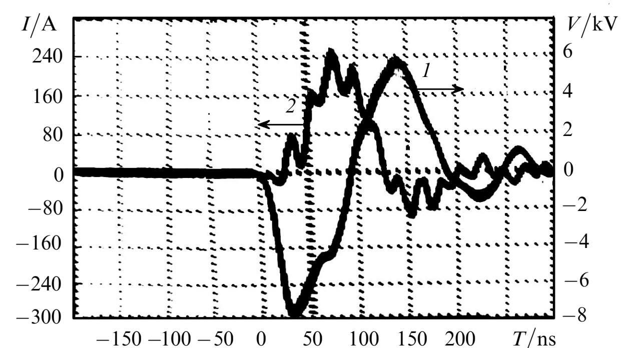

Figure 6. Voltage (*1*), current (*2*) and laser (*3*) pulses for 13-mm bore, 30-cm long CuCl-laser tube at a Ar buffer gas pressure of 10 Torr.

larger, which leads to high energy losses during each collision.

Due to these reasons, the use of He as a buffer gas does not produce suitable electron distribution because low-energy electrons in plasma populate the lower energy levels and deteriorate the laser operation.

If Ar is used as a buffer gas, the peak current significantly increases to 240 A. This indicates the reduction in the plasma tube resistance caused by the lower ionisation potential of Ne (15.76 eV) and higher atomic weight compared to He. The decrease in plasma tube resistance results in a considerable impedance mismatch between the plasma tube and the external circuit. The oscillation in voltage and

current waveform in Fig. 6 confirms this statement. One can see that the maximum current occurs at a very low voltage level, so there are a lot of low-energy electrons in the tube which can spoil laser operation.

3.2 Copper chloride vapour pressure

One of the most important parameters for laser optimisation is the CuCl vapour pressure. It was found in this research that when the distance between the discharge axis and CuCl source is 10 cm, it is possible to control the vapour pressure through the external heater independently of discharge temperature. Figure 7 shows the dependence of the average output power on the CuCl vapour pressure.

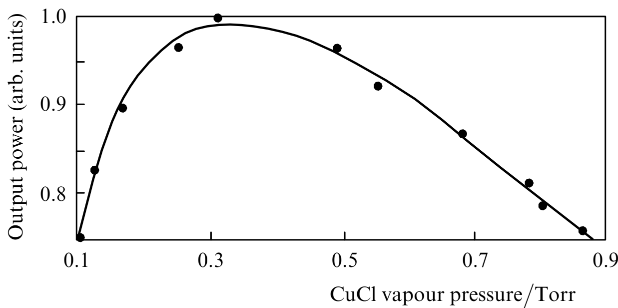

Figure 7. Dependence of the average output laser power on the CuCl vapor pressure at a Ne buffer gas pressure of 30 Torr.

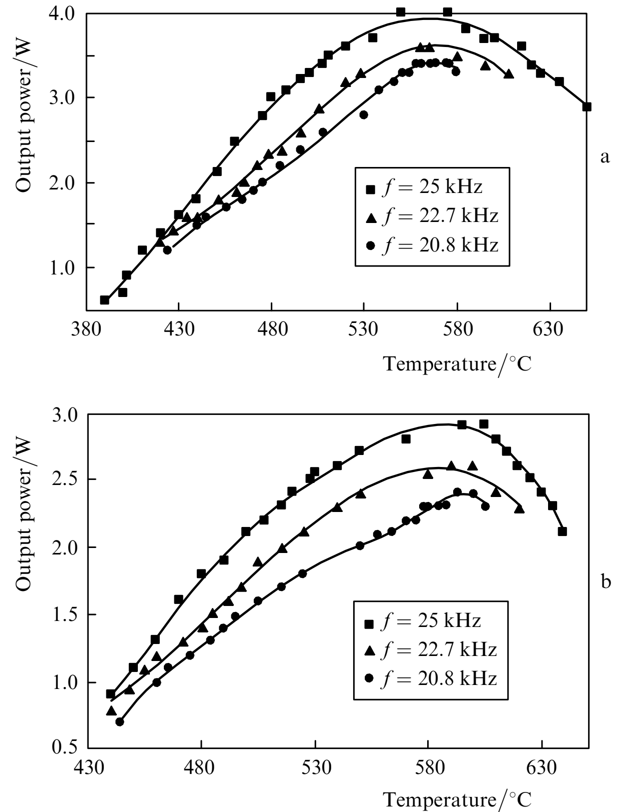

Figure 8. Dependences of the average output power on the tube wall temperature for different pulse repetition rates and diaphragm diameters of 13 (a) and 10 mm (b).

4. Optimisation of a laser to a specified output power

The circuit and switch parameters being optimised, we measured the specific output power by using two types of diaphragms under the optimum operation condition (the Ne pressure of 30 Torr and the CuCl pressure of 0.3 Torr). At first, four diaphragms with internal diameter of 13 mm were installed inside the discharge tube. In this case the active volume decreased down to 40 cm^3. In this configuration, we measured the dependence of the average output power on the tube wall temperature at different pulse repetition rates. The results are presented in Fig. 8. This diagram indicates that the optimal operation temperature of the tube is about of 560 °C. One can also see that the highest output power of 4 W was achieved for a pulse repetition rate of 25 kHz and the average input power of 9 W cm^{-3} (including electrodes and circuit losses), which corresponds to the average specific output power of 100 W L^{-1}.

Under the same condition, we installed quartz diaphragms with the diameter of 10 mm and the active volume decreased down to 23.5 cm^3. The average output power was measured as a function of the tube wall temperature for different pulse repetition rates. The results of the measurements are presented in Fig. 8b. One can see that when these diaphragms were used, the optimum operation temperature increased to 600 °C. Under these conditions, the maximum output power of 2.9 W was achieved for a pulse repetition rate of 25 kHz and the input power of 12 W cm^{-3} (including electrodes and circuit losses), which corresponds to the specific output power of 123 W L^{-1}.

4.1 Radial profile of the gas plasma temperature

It is known that diaphragms cause the change in the radial profile of gas plasma temperature in active medium [9]. The cross section of the discharge tube is shown in Fig. 9. Diaphragms separate the tube interior in two regions. The electric discharge is located in region I with radius R_1. The power input is considered to be uniform in this region. In region II located between diaphragms and the tube wall ($R_1 < r < R_2$), the power deposition is zero.

The steady-state heat equation is

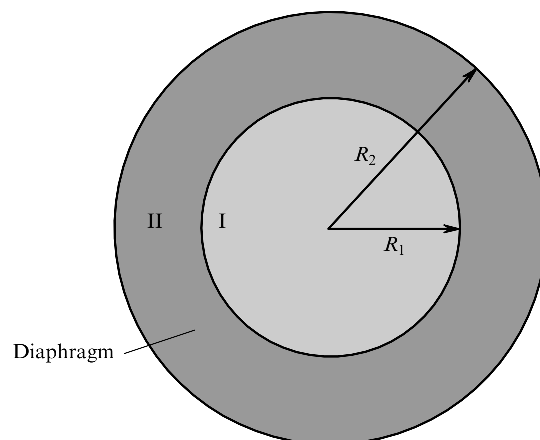

Figure 9. Cross section of the discharge tube with diaphragms.

$$\vec{\nabla}(S\vec{\nabla}T) + P_v = 0, \quad (1)$$

where S is the thermal conductivity; T is the gas temperature; P_v is the power deposited in region I per unit volume. By assuming that the gas temperature varies only in the radius direction, Eqn (1) transforms to

$$\frac{1}{r}\frac{\mathrm{d}}{\mathrm{d}r}\left(rS\frac{\mathrm{d}T}{\mathrm{d}r}\right) + P_v = 0. \quad (2)$$

The temperature dependence of the thermal conductivity of the Ne buffer gas has the form [24]

$$S = 9.7 \times 10^{-4} T^{0.685}. \quad (3)$$

By considering the boundary condition on the wall and in the centre of the tube and assuming the continuity of the temperature distribution, the solution of (2) has the form for region II

$$T_2(r) = \left(T_{\mathrm{w}}^{1.685} + \frac{1.685}{2 \times 9.7 \times 10^{-4}} P_v R_1^2 \ln\frac{R_2}{r}\right)^{0.593}. \quad (4)$$

And for region I

$$T_1(r) = \left[T_{\mathrm{b}}^{1.685} + \frac{1.685}{4 \times 9.7 \times 10^{-4}} P_v (R_1^2 - r^2)\right]^{0.593}, \quad (5)$$

where

$$T_{\mathrm{b}} = \left(T_{\mathrm{b}}^{1.685} + \frac{1.685}{2 \times 9.7 \times 10^{-4}} P_v R_1^2 \ln\frac{R_2}{R_1}\right)^{0.593}; \quad (6)$$

and T_{w} is the tube wall temperature.

The solution of these equations allows us to obtain the radial profile of the gas plasma temperature under different conditions. The results of these calculations are shown in Fig. 10.

Curve (*1*) in Fig. 10 illustrates the temperature dependence in the tube cross section of diameter 20 mm without using any diaphragms. In this case, the temperature of plasma gas varies from 2340 K on the central axis to 863 K on the tube wall. The temperature of the reservoir was 693 K. Because of the low electron and gas temperature near the tube wall, the dissociation of CuCl molecules, excitation and population inversion of Cu atoms are confined to central regions. Thus, it is impossible to use all the volume of tube as an active medium, which leads to a decrease in the specific output power. In addition, it is impossible to increase the tube wall temperature, much more, because of the heat tolerance of fused silica.

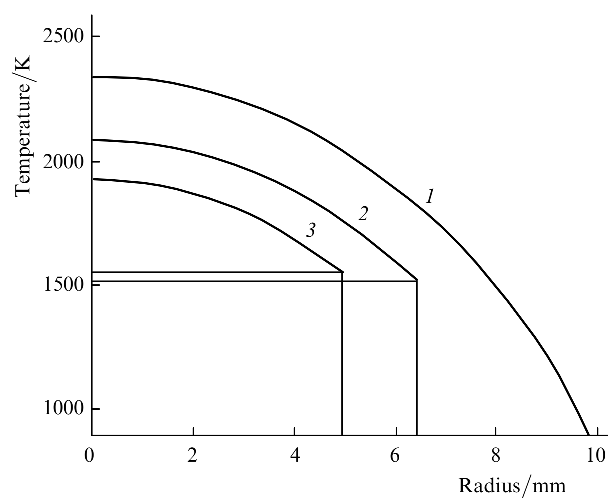

Figure 10. Radial profile of the gas plasma temperature in the cross section for the internal diameter of 20 mm (without diaphragms) and the input power density of 9 W cm^{-3} (*1*), with the diaphragms of the diameter 13 mm and the input power density of 9 W cm^{-3} (*2*) and with the diaphragms of the diameter 10 mm and the input power density of 10 W cm^{-3} (*3*).

The temperature profile for the 13-mm diaphragms and for the optimum operation temperature of tube walls (560 °C) is shown by curve (*2*). One can see that the radial temperature profile became more uniform. The gas plasma temperature varies from 2085 K on the central axis of region I to 1513 K on its border. Thus, under these conditions, the high-energy electrons can be found at any distance from the centre.

Curve (*3*) in Fig. 10 shows the temperature profile for the 10-mm diaphragms and for optimum operation temperature of tube walls (600 °C). The gas plasma temperature varies from 1929 K on the central axis of region I to 1545 K on its border. To achieve this profile, one needs to increase the average specific input power up to 12 W cm^{-3}. Under these conditions, the specific output power is 123 W L^{-1}. In this case, the radial profile of gas plasma temperature was much more uniform than that in the previous case. This allows one to increase the number of high-energy electrons in the entire volume and thus to raise the specific output power.

5. Conclusions

We have optimised the specific output power of the CuCl laser by adjusting the permissible current rise rate of the thyratron and changing the crucial parameters of the buffer

Table 1.

Active medium	Internal diameter of the tube/mm	Tube length/cm	Output power/W	Specific output power/W L^{-1}	References
CuCl	11	40	3	79	[23]
CuCl	18	90	6.3	27.5	[24]
CuCl	25	100	12.5	25.5	[25]
CuCl	18	55	13.2	94	[26]
CuBr	18	55	13.2	94	[26]
CuI	12	45	2.6	51	[27]
CuCl	30	70	18.5	37	[28]
CuBr	22	75	3.6	12.6	[24]
CuBr	20	50	3.2	20	[29]
CuBr	12	45	2.1	41	[30]
CuBr	20	60	4.2	22	[30]
CuBr	22	75	7.8	27	[30]
CuBr	20	65	17.5	85.7	[31]
CuBr	20	50	6	38	[13]
CuBr	20	50	5.3	33.8	[32]
CuCl	20	50	3.5	22.3	[32]
CuBr	25	80	11	28	[33]
CuBr	13	33	3.5	80	[22]
CuCl	10	30	2.9	123	This paper
CuCl	13	30	4	100	This paper

gas and copper chloride vapour pressure and also by confining the active region with quartz diaphragms. The dependence of the specific output power on the temperature profile has been investigated. These results have obtained by assuming that the wall temperature does not affect the CuCl vapour pressure, because it is controlled by the external heater. Thus, the dependence of the specific output power on the wall temperature demonstrates its dependence on the radial profile of the gas plasma temperature. In our experiment, the maximum specific output powers of 100 and 123 W L^{-1} have been achieved with diaphragms having the internal diameter of 14 and 10 mm, respectively. Table 1 shows the results of experiments performed by a number of researchers. One can see that the specific output power reported in this work is the highest one among all the existing copper halide lasers without any admixtures like hydrogen.

Acknowledgements. The authors thank Mr. Khorasani and Mr. Salehinia for the construction of the power supply and Mr. Kia for his help in this project.

References

1. Walter W.T. , Solimen N., Piltch M., Gould G. *IEEE J. Quantum Electron.*, **2**, 474 (1966).
2. Iseki Y., Watanabe I., Nona E. *Jpn. J. Appl. Phys.*, **41**, 5181 (2002).
3. Batanin V.M., Generalov N.A. *Kvantovaya Elektron.*, **35**, 484 (2005) [*Quantum Electron.*, **35**, 484 (2005)].
4. Lyabin N.A., Chursin A.D., Ugol'nikov S.A., Koroleva M.E., Kazaryan M.A. *Kvantovaya Elektron.*, **31**, 191 (2001) [*Quantum Electron.*, **31**, 191 (2001)].
5. Ohzu Akira, Kato Masaaki, Maruyama Yolchiro. *Rev. Sci. Instr.,* **71**, 2228 (2000).
6. Chang T., Alger T.W., et al. *Conf. Lasers and Electrooptics CLEO' 1994* (Anaheim, CA, 1994).
7. Chang C. *J. Phys. D: Appl. Phys.*, **33**, 1169 (2000).
8. Boichenko A.M., Evtushenko G.S., Zhdaneev O.V., Yakovlenko S.I. *Kvantovaya Elektron.*, **35**, 578 (2005) [*Quantum Electron.*, **35**, 578 (2005)].
9. Zemskov K.I., Isaev A.A., Petrash G.G. *Kvantovaya Elektron.*, **27**, 183 (1999) [*Quantum Electron.*, **29**, 462 (1999)].
10. Saito H., Shiraiwa Y., Ishiicawa T. *Appl. Phys. Lett.,* **78**, 2113 (2001).
11. Carman R.Y., Brown D.J.W., Piper J.A. *IEEE J. Quantum Electron.*, **30**, 1876 (1994).
12. Astadjov D.N., Sabotinov N.V., Vuchkov N.K. *IEEE J. Quantum Electron.*, **24**, 1927 (1988).
13. Astadjov D.N., Isaev A.A., Petrash G.G., Ponomarev I.V., Sabotonov N.V., Vuchkov N.K. *IEEE J. Quantum Electron.*, **28**, 1966 (1992).
14. Sabotinov N.V., Vuchkov N.K., Astadjov D.N. *Opt. Gommun.*, **95**, 55 (1993).
15. Boichenkov A.M., Evtushewko G.S., Zhdaneev O.V., Yakovlenko S.I. *Kvantovaya Elektron.*, **33**, 1047 (2003) [*Quantum Electron.*, **33**, 1047 (2003)].
16. Sabotinov N.V., Dimitrov K.D., Vuchkov N.K., Astadjov D.N., Kirkov V.K., Little C.E., Jones D.R. *Techn. Dig. Conf. CLEO Europe* (Hamburg, Germany, 1996) p. 6.
17. Yudin N.A. *Kvantovaya Elektron.*, **25**, 795 (1998) [*Quantum Electron.*, **28**, 774 (1998)].
18. Yudin N.A. *Kvantovaya Elektron.*, **32**, 815 (2002) [*Quantum Electron.*, **32**, 815 (2002)].
19. Astadjov D.N., Dimitrov K.D., Little C.E., Sabotinov N.V., Vuchkov N.K. *IEEE. J. Quantum Electron.*, **30**, 1358 (1994).
20. Sadighi-Bonabi R., Lee F.W., Collins C.B. *J. Appl. Phys.*, **53**, 8508 (1982).
21. Sadighi-Bonabi R. *PhD Thesis* (Dallas, University of Texas, 1983).
22. Little C.E. *Metal Vapor Lasers* (New York: John Wiley & Sons, 1999).
23. Isaev A.A., Kazaryan M.A., Lemmerman G.Yu. *Kvantovaya Elektron.*, **3**, 1800 (1976) [*Sov. J. Quantum Electron.*, **6**, 976 (1976)].
24. Markova S.V., Petrash G.G., Cherezov V.M. *Proc. Lebedev Phys. Inst.*, **181** (Nova Science Commack, 1989) p. 23.
25. Nerheim N.M., Bhanji A.M., Russell G.R. *IEEE J. Quantum Electron.*, **14** (9), 686 (1978).
26. Kazaryan M.A., Petrash G.G., Trofimov A.N. *Kvantovaya Elektron.*, **7**, 583 (1980) [*Sov. J. Quantum Electron.*, **10**, 328 (1980)].
27. Andrews A.J., Tobin R.C., Webb C.E. *J. Phys. D: Appl. Phys.*, **13**, 1017 (1980).
28. Abas-Ogly Ya.R., Aboyan S.A., Abrosimov G.V. *Kvantovaya Elektron.*, **8**, 648 (1981) [*Sov. J. Quantum Electron.*, **11**, 391 (1981)].
29. Astadzhov D.N., Vuchkov N.K., Petrash G.G. *Kvantovaya Elektron.*, **14**, 396 (1987) [*Sov. J. Quantum Electron.*, **17**, 245 (1987)].
30. Trofimov A.N. *Cand. Diss.* (Moscow, 1982).
31. Marazov O.R., Manev E.G. *Opt. Commun.*, **78** (1), 63 (1990).
32. Sabotinov N.V., Vuchkov N.K., Astadjov D.N. *Opt. Commun.*, **95**, 55 (1993).
33. Isaev A.A., Petrash G.G., Little C.E., Jones D.R. *IEEE J. Quantum Electron.*, **33** (6), 919 (1997).